

# Theoretical and Observational Assessments of Flare Efficiencies

**Douglas M. Leahey and Katherine Preston**

*Jacques Whitford Environment Limited, Calgary, Alberta, Canada*

**Mel Strosher**

*Alberta Research Council, Calgary, Alberta, Canada*

## ABSTRACT

Flaring of waste gases is a common practice in the processing of hydrocarbon (HC) materials. It is assumed that flaring achieves complete combustion with relatively innocuous byproducts such as CO<sub>2</sub> and H<sub>2</sub>O. However, flaring is rarely successful in the attainment of complete combustion, because entrainment of air into the region of combusting gases restricts flame sizes to less than optimum values. The resulting flames are too small to dissipate the amount of heat associated with 100% combustion efficiency.

Equations were employed to estimate flame lengths, areas, and volumes as functions of flare stack exit velocity, stoichiometric mixing ratio, and wind speed. Heats released as part of the combustion process were then estimated from a knowledge of the flame dimensions together with an assumed flame temperature of 1200 K. Combustion efficiencies were subsequently obtained by taking the ratio of estimated actual heat release values to those associated with 100% complete combustion.

Results of the calculations showed that combustion efficiencies decreased rapidly as wind speed increased from 1 to 6 m/sec. As wind speeds increased beyond 6 m/sec,

combustion efficiencies tended to level off at values between 10 and 15%. Propane and ethane tend to burn more efficiently than do methane or hydrogen sulfide because of their lower stoichiometric mixing ratios.

Results of theoretical predictions were compared to nine values of local combustion efficiencies obtained as part of an observational study into flaring activity conducted by the Alberta Research Council (ARC). All values were obtained during wind speed conditions of less than 4 m/sec. There was generally good agreement between predicted and observed values. The mean and standard deviation of observed combustion efficiencies were  $68 \pm 7\%$ . Comparable predicted values were  $69 \pm 7\%$ .

## INTRODUCTION

Flares are routinely employed in the chemical and petroleum industries for the disposal of large quantities of unwanted flammable gases and vapors. Byproducts of the flaring process are usually assumed to be entirely composed of relatively innocuous gases such as CO<sub>2</sub> and H<sub>2</sub>O. Evidence presented by flare manufacturers demonstrates that the flaring process is an efficient destruction mechanism for the original components of feed gases.<sup>1</sup> Thus, for example, very little CH<sub>4</sub> is measured downwind from CH<sub>4</sub>-fueled flares. However, few studies appear to confirm that the conversion is to H<sub>2</sub>O and CO<sub>2</sub> rather than to gases with more complex molecular structures such as polycyclic aromatic hydrocarbons and volatile organic compounds, which are indicative of incomplete combustion. There seems to have been little motivation to conduct such studies because they are expensive and because flares have appeared to be a reliable conversion mechanism.

The U.S. Environmental Protection Agency (EPA) has reported that "properly operated flares achieve at least 98% combustion efficiency in the flare plume."<sup>2</sup> According to EPA, this relatively high efficiency is achieved by a fuel value in the flared gases of at least 7500–9300 kJ/m<sup>3</sup>

## IMPLICATIONS

Flares are used extensively to dispose of gaseous wastes. The usual assumption is that combustion processes associated with flares efficiently convert HCs and sulfur compounds to relatively innocuous gases such as CO<sub>2</sub>, SO<sub>2</sub>, and H<sub>2</sub>O. It has been shown, however, that these processes can be efficient only at low wind speeds because the size of the flare flame, which is an indicator of flame efficiency, decreases with increasing wind speed. Therefore, the flaring process could routinely result, during periods of moderate to high wind speeds, in appreciable quantities of products of incomplete combustion such as anthracene and benzo(a)pyrene, which can have adverse implications with respect to air quality.

and by having sufficient fuel-air mixing to provide at least the stoichiometric amount of oxygen to achieve and maintain high flame temperatures. There is no suggestion that combustion efficiencies may depend on parameters that influence flame size, and consequently heat releases, such as stack exit velocities and wind speeds.

Ideally, theoretical studies of flame efficiencies should be based upon knowledge of the full range of chemical reactions and associated kinetics. Such an analysis, which is almost always difficult, is made more intractable for the case of flares because the combustion chamber (that is, flame volume) is a function of such variables as wind speed and stack exit velocity.<sup>3,4</sup> Fortunately, there is a simpler method for calculating the combustion efficiency of a flare that does not depend upon a detailed knowledge of chemical reactions. It relies instead upon the law of energy conservation, whereby the heat of combustion released within the flame must be balanced by sensible heat gains and radiational losses

$$H_f = S + R' \quad (1)$$

where  $H_f$  is the rate of heat released from combusting gases within the flame (J/sec),  $S$  is the rate of sensible heat gain by the air as it passes through the volume of the flame (J/sec), and  $R'$  is the rate of radiational heat loss by flame (J/sec). Complete combustion will only be achieved if  $S + R'$  equals the heat content of the flared gases. Estimates of this sum require knowledge of the flame dimensions and an understanding of its radiation temperature.

It has long been recognized that knowledge of flame behavior is useful in estimating its radiation characteristics.<sup>5-7</sup> Leahey et al.<sup>8</sup> have pointed out that a means of predicting the size of the diffusion flame could also be useful in estimating its combustion efficiency. This is because more air is entrained into large flames than into small flames, and consequently more oxygen is available and more heat can be dissipated by large flames, resulting in greater combustion efficiency. If a flame's dimensions are dependent, for example, on meteorological variables, so must be the efficiency with which the flame combusts fuel.

Appreciable work has been done on the empirical evaluation of flame shapes and sizes.<sup>3,9-16</sup> Much of the work has resulted in methods to predict gross features of the flame such as the distance from the flame tip to the burner tip. Perhaps the most widely used empirical method for predicting this length is the one proposed by Brzustowski,<sup>3,4</sup> which has some theoretical foundation. Its accuracy is to within a factor of 2.

Leahey et al.<sup>8</sup> have developed a theoretical model for flame behavior that may be used to predict flame dimensions including length, diameter, area, and volume. It includes the effects of air entrainment into the flame and

conserves both momentum and mass. The model is based on the assumption, following the theoretical findings of Escudier<sup>17</sup> and observational results of Becker et al.,<sup>18</sup> that the effects of buoyancy forces on flame behavior are negligible. Observational assessments have shown that predictions of the Leahey and Schroeder model agree well with actual flame dimensions for a sour gas flare;<sup>8,19</sup> for methane, propane, ethylene, and butane flames observed in a wind tunnel;<sup>20</sup> and for a very large emergency flare.<sup>21</sup> One-to-one correlations between predicted and observed flame parameters were ~0.90.

Temperatures associated with the combustion of hydrocarbons (HCs) such as methane, propane, and butane are observed in furnaces to be ~1900 °C.<sup>22</sup> These values, however, are not relevant to flare flames, which are subjected to greater cooling effects of wind and radiation than are furnace fires. Theoretical considerations show that comparable HC flare temperatures may be as low as 1100 °C.<sup>15,23</sup> Detailed laboratory measurements of temperatures associated with a propane flame in calm winds showed them to be ~1000 °C.<sup>10</sup> These were observed to increase to ~1200 °C as winds and stack exit velocities increased. Such behavior was opposite to that observed by Leahey et al.,<sup>8</sup> who found that average radiation temperatures during field tests of an industrial flare decreased from ~1025 to 875 °C as wind speeds increased from 1.5 to 3.0 m/sec, respectively. The average temperature observed by Leahey et al.<sup>8</sup> was ~925 °C.

A series of observational studies into combustion efficiencies associated with flaring activity at oil battery sites was recently completed by the Alberta Research Council (ARC).<sup>24,25</sup> They consisted of measuring carbon- and sulfur-based compounds in the region immediately downwind of diffusion flares. The results of the data analyses agreed with prior studies insofar as they showed that the feed gases (such as methane and ethane) to the flare were largely destroyed. However, they also showed that pyrolysis converted significant quantities of these feed gases to many complex chemical species such as benzo(a)pyrene, naphthalene, and phenylthiophene rather than simply to CO<sub>2</sub>, SO<sub>2</sub>, and H<sub>2</sub>O, which would be the sole products of complete combustion. This paper presents equations for predicting flare efficiencies and compares theoretical estimates with values obtained from observational studies conducted by the ARC.

## THEORY

The rate at which heat is generated by fuel combustion within a diffusion flame is shown in eq 1 as the sum of the rates at which sensible heat ( $S$ ) is being gained by the air and radiational heat ( $R'$ ) is being lost by the flame. The value of  $S$  was calculated by assuming that air receives heat only as it passes through the volume of the flame. The time,  $t_p$ , taken for air to travel the length of the plume was assumed to be  $x_f/U$ ,

where  $x_f$  and  $U$  are the length of the plume and wind speed, respectively. Values of  $S$  are then given by the heat gained by air occupying the flame volume over  $t_f$

$$S = \frac{C_p \rho_f V_f (T_f - T_o)}{t_f} \quad (\text{J/sec}) \quad (2)$$

where  $C_p$  is the specific heat of air at constant pressure (1010 J/kg/K);  $\rho_f$  is the air density at flame temperature (kg/m<sup>3</sup>);  $V_f$  is the volume of the flame (m<sup>3</sup>);  $T_f$  is the flame temperature (K);  $T_o$  is the ambient temperature (K);  $t_f$  is the time over which air passes through the flame ( $x_f/U$ );  $x_f$  is the horizontal length of the flame (m); and  $U$  is the wind speed (m/sec). Values of  $V_f$  and  $x_f$  may be calculated using equations associated with the Leahey and Schroeder model as presented in the Appendix. These equations are functions of wind speed, exit gas velocity, and stoichiometric mixing ratio.

Radiational heat loss was estimated using the Stefan-Boltzmann relation for a black body

$$R' = A_f \sigma T_f^4 \quad (\text{J/sec}) \quad (3)$$

where  $A_f$  is the area of flame (m<sup>2</sup>) and  $\sigma$  is the Stefan-Boltzmann constant ( $5.67 \times 10^{-8}$  J/sec/m<sup>2</sup>/K<sup>4</sup>). An examination of eq 3 shows that radiational heat loss is very sensitive to flame temperature. A relatively small decrease in temperature from 1250 to 1200 K (977 to 927 °C), for example, will decrease heat loss by 15%.

An equation for calculating  $A_f$  as a function of the stack exit velocity, wind speed, stack exit temperature, ambient temperature, and stoichiometric mixing ratio is given in the Appendix. The stoichiometric air/fuel ratio in this context refers to the proportion of the constituents of the reactants in air such that there are exactly enough molecules of oxygen to bring about a complete reaction to stable molecular forms in the products. It is usually expressed in units of %.

Estimates of combustion efficiencies ( $E$ ) may be obtained by comparing flame heat loss ( $H_f$ ) to the heat ( $H$ ) that would have been released if the combustion of all flare gases went to completion (i.e., CO<sub>2</sub>, SO<sub>2</sub>, and H<sub>2</sub>O)

$$E = \frac{100 H_f}{H} \quad (\%) \quad (4)$$

where  $E$  is the combustion efficiency of flame (%);  $H$  is  $H_1 Q$  (J/sec);  $H_1$  is the heat content of flared gases (J/m<sup>3</sup>); and  $Q$  is the release rate of gases (m<sup>3</sup>/sec). In addition,

$$Q = \frac{\pi D_o^2 V}{4} \quad (5)$$

where  $D_o$  is the stack diameter (m) and  $V$  is the stack exit velocity (m/sec). Values of  $E$  equal to or greater than 100% indicate a flame size consistent with complete combustion.

For purposes of simplicity, it is assumed that the heat released by an incomplete combustion reaction will be less than the heat released by a complete combustion reaction. The calculated heat content or heating value,  $H_f$ , assumes that there is excess oxygen, so combustion goes to completion. The heating value is dependent on the heat of formation of products and reactants. Carbon dioxide is a very stable form of carbon and, as such, has a large heat of formation relative to other carbon compounds with a lower oxidation state. Thus, for instance, less heat is released when an HC is combusted to CO and other products than when it is combusted to CO<sub>2</sub> and H<sub>2</sub>O. Nonetheless, there may be exceptions to this rule whereby more heat is released by a complex incomplete combustion reaction than by the corresponding complete combustion reaction.

An examination of eqs 1–4 together with the expressions for flame dimensions contained in the Appendix showed that estimated flame efficiencies will not be a function of flare stack diameters. Equations 1–4 were applied to evaluate combustion efficiencies associated with the burning of methane, ethane, propane, and hydrogen sulfide for flare stacks with gas exit velocities of 2.0, 10.0, and 25.0 m/sec under a wide range of assumed wind speed conditions. The stoichiometric mixing ratios for these gases are 9.5, 5.7, 4.0, and 12.3%, respectively. The corresponding heating values are 34, 60, 86, and 22 MJ/m<sup>3</sup>. For purposes of estimating combustion

**Table 1.** Estimated combustion efficiencies (%) for the indicated gases as functions of stack exit velocity  $V$  (m/sec) and wind speed  $U$  (m/sec).

$U$ (m/sec)	Methane	Ethane	Propane	Hydrogen Sulfide
<b><math>V = 2.5</math> m/sec</b>				
2	52.7	79.7	111.1	50.3
5	28.3	41.3	65.1	27.6
10	17.6	24.5	32.7	17.7
15	13.7	18.3	23.9	14.1
20	11.7	15.1	19.3	12.2
<b><math>V = 10</math> m/sec</b>				
2	30.4	44.7	61.3	29.6
5	21.4	30.4	41.0	21.2
10	15.3	20.8	27.5	15.6
15	12.5	16.5	21.3	13.0
20	11.0	14.0	17.8	11.5
<b><math>V = 20</math> m/sec</b>				
2	20.7	29.4	39.6	20.6
5	16.7	24.5	30.7	16.9
10	13.3	17.6	22.9	13.7
15	11.4	14.7	18.8	11.9
20	10.2	12.9	16.2	10.9

efficiencies, it was assumed, based upon field flare measurements as reported by Leahey et al.,<sup>8</sup> that flame temperatures would average 1200 K.

Table 1 presents combustion efficiencies for methane, ethane, propane, and hydrogen sulfide as calculated through eq 4 for the indicated ranges of wind speed and stack exit velocities. Values for  $H_i$  as contained in eq 4 were obtained from eq 1 using the values of  $S$  and  $R'$  presented in eq 3 and eq 4 together with equations for flame dimensions (length, area, volume), as given in the Appendix. The table shows that  $\text{CH}_4$  and  $\text{H}_2\text{S}$  flares tend to be relatively inefficient as compared with ethane and especially propane flares. This is because  $\text{CH}_4$  and  $\text{H}_2\text{S}$  have larger stoichiometric ratios, so their flame sizes tend to be smaller and less able to dissipate heat. As shown in Table 1, combustion efficiencies are predicted to decrease with increasing wind speeds and exit velocities. With wind speeds of 20 m/sec, predicted efficiencies tend to be in the 10–15% range.

### OBSERVATIONAL STUDIES

The ARC conducted field measurements of products of incomplete combustion downwind of flare plumes at a sweet oil battery site (no  $\text{H}_2\text{S}$  in the flared gas) and a sour oil battery site (23%  $\text{H}_2\text{S}$  in the gaseous stream directed to flare). The flare system at the sweet oil battery site consisted of a liquid knockout drum and a freestanding flare stack 12 m in height and 20 cm in diameter at the top. It was equipped with an auto-igniter and a wind deflector to prevent flare blowout. The flare system at the sour oil battery site was similar to that at the sweet oil battery site. Stack height and diameter were 15 m and 7.6 cm, respectively. The percentages of flammable compositions for the gases combusted at each flare site are presented in Table 2. In both cases, the largest component of the noncombusted gas was  $\text{CH}_4$ . Table 2 also presents values of the heat content and stoichiometric mixing ratios.

Table 3 presents stack, emission, and measured plume parameters for the sweet and sour flares studied by the ARC. As the stack diameter and exit velocity for the sweet gas flare were significantly larger than those for the sour gas flare, the effluent gas volume for the sweet gas flare was correspondingly much greater. Downwind distances to the measurement point from the flare stack outlet were about twice the flame length. The plume temperatures shown in Table 3 are those measured at the indicated downwind distance. No measurements were made of actual flame temperatures.

A single probe sampling system was developed and tested in the laboratory prior to field sampling. Standard HC mixtures were directed through the heated probe

**Table 2.** Percent flammable composition of gas combusted at the two observed flare sites. Heating value of each gas ( $\text{MJ}/\text{m}^3$ ) and stoichiometric mixing ratios are also shown.

Component	Sweet Gas Flare	Sour Gas Flare
Butane	4.6	2.4
Ethane	9.2	10.7
Hydrogen sulfide	0.0	22.8
Methane	69.2	45.4
Pentane	8.6	2.6
Propane	5.5	5.7
Heating value ( $\text{MJ}/\text{m}^3$ ) <sup>a</sup>	51.3	38.5
Stoichiometric mixing ratios (percent)	6.4	7.7

<sup>a</sup>At 288 K and 101.325 kPa.

and heat-traced lines of varying temperatures to determine the most suitable temperature for HC recovery. The sampling system was fitted to a hydraulic basket lift with a 20-m reach. The probe was attached to a boom that was in turn fastened to the basket. Samples were collected at several locations along the length of the sampling system, which included the sampling probe, a short length of heated sampling line that reached to the basket level, and a longer length of heated sampling line that extended to the ground. Samples were collected immediately after the probe, at the basket level, and at ground level. They were drawn from this sampling system for the analyses either by on-site analytical equipment or through absorbent samplers for confirmatory analyses by combined gas chromatography/mass spectrometry. More details of sampling procedures and analytical techniques can be found elsewhere.<sup>24,25</sup>

Estimates of local combustion efficiencies ( $CE$ ) consistent with measured HC and sulfur species were obtained

**Table 3.** Stack, emission, and measured plume parameters associated with the two gas flares sampled.

Parameter	Sweet Gas Flare	Sour Gas Flare
Stack height (m)	12.0	15.0
Stack diameter (m)	0.2	0.076
Stack exit velocity (m/sec)	3.2	1.65
Gas effluent rate ( $\text{m}^3/\text{sec}$ ) <sup>a</sup>	0.1000	0.0075
Ambient temperature (K)	288	288
Flame length (m)	4.5	1.75
Measured plume temperature (K)	373	398
Wind speed (m/sec)	1.9	2.0
Total measurement time (min)	40	80
Measurement time in plume (m)	30	60
Downwind distance to measurement point (m)	9.0	3.5

<sup>a</sup>At 288 K and 101.325 kPa.

**Table 4.** Speciated data for combustion products observed downwind of the sweet gas flare using solvent extraction methods (mg/m<sup>3</sup>).

Compound	Amount
Nonane	0.41
Benzaldehyde (acn)(dot)	0.53
Benzene, 1-ethyl-2-methyl-	0.13
1h-indene, 2,3-dihydro-	0.34
Decane	1.72
Benzene, 1-ethynyl-4-methyl-	9.83
Benzene, 1,3-diethenyl-	1.27
1h-indene, 1-methylene-	0.28
Azulene	21.20
Benzene, (1-methyl-2-cyclopropen-1-yl)-	11.47
1h-indene, 1-methyl-	1.66
Naphthalene (can)(dot)	99.39
Benzaldehyde, o-methyloxime	0.27
1-h-inden-1-one, 2,3-dihydro-	0.74
Naphthalene, 2-methyl-	9.25
Naphthalene, 1-methyl-	6.18
1h-indene, 1-ethylidene-	1.22
1,1'-biphenyl	58.70
Naphthalene, 2-ethyl-	1.87
Biphenylene	42.81
Naphthalene, 2-ethenyl-	7.32
Acenaphthylene	7.15
Acenaphthene	2.93
Dibenzofuran	0.88
1,1'-biphenyl, 3-methyl-	0.31
1h-phenalene	21.01
9h-fluorene	41.09
9h-fluorene, 9-methyl-	1.07
Benzaldehyde, 4,6-dihydroxy-2,3-dimethyl	1.16
9h-fluorene, 9-methylene-	1.07
9h-fluorene, 3-methyl-	3.05
Phenanthrene	10.01
Benzo(c)cinnoline	2.06
Anthracene	42.11
1h-indene, 1-(phenylmethylene)-	1.94
9h-fluorene, 9-ethylidene-	0.89
1h-phenalen-1-one	1.86
4h-cyclopenta[def]phenanthrene	3.50
Naphthalene, 2-phenyl-	1.98
Naphthalene, 1-phenyl-	1.82
9,10-anthracenedione	0.94
5h-dibenzo[a,d]cycloheptene, 5-methylene-	0.75
Naphthalene, 1,8-di-1-propynyl-	1.14
Fluoranthene	51.35
Benzene, 1,1'-(1,3-butadiyne-1,4-diyl)bis-	2.07
Pyrene	32.37
11h-benzo[a]fluorene	2.25
Pyrene, 4-methyl-	9.13
Pyrene, 1-methyl-	8.38
Benzo[ghi]fluoranthene	10.16
Cyclopenta[cd]pyrene	29.77
Benzo[a]anthracene	17.33
Chrysene	2.12
Benzene, 1,2-diphenoxy-	1.94
Methanone, (6-methyl-1,3-benzodioxol-5-yl)phenyl-	0.95
Benzo[e]pyrene	0.71
Benzo[a]pyrene	1.03
Perylene	0.62
Indeno[1,2,3-cd]pyrene	0.15
Benzo[ghi]perylene	0.26
Dibenzo[def,mno]chrysene	0.15
Coronene	0.08

through the following equations, which employ the carbon/sulfur equivalents of each detected gas:

$$CE (\%) = \frac{C(\text{CO}_2)100}{C(\text{CO}_2) + C(\text{CO}) + C(\text{HC}) + C(\text{soot})} \quad (6)$$

$$CE (\%) = \frac{S(\text{SO}_2)100}{S(\text{SO}_2) + S(\text{H}_2\text{S}) + S(\text{COS}) + S(\text{CS}_2) + S(\text{S compounds})} \quad (7)$$

where  $C(\text{CO}_2)$ ,  $C(\text{CO})$ ,  $C(\text{HC})$ , and  $C(\text{soot})$  are the number of carbon atoms existing in the form of  $\text{CO}_2$ ,  $\text{CO}$ ,  $\text{HC}$ , and soot, respectively. Equation 7 is similar to eq 6 except that it is formulated in terms of sulfur rather than carbon.

Table 4 presents an example of the speciated data for combustion products observed downwind of the sweet gas flare when the wind speed and stack exit velocity were 1.7 and 3.2 m/sec, respectively. The estimated associated combustion efficiency was 65%. These components are representative of the hydrocarbons identified during other tests with similar values of wind speed and exit velocity.

#### COMPARISON BETWEEN THEORETICAL PREDICTIONS AND OBSERVATIONAL RESULTS

There were a total of nine observational tests, which allowed for the estimation of local combustion efficiencies. Table 5 shows the wind speeds and stack exit velocities associated with each test. The flare during the first test had a very low stack exit velocity of only 0.8 m/sec. Stack exit velocities during other tests conducted on the sweet gas flare (tests 2–8) were similar, with an average value of 3.1 m/sec. The final test (test 9), which was conducted on the sour gas, was associated with a stack exit velocity of 1.7 m/sec.

Figure 1 shows theoretical combustion efficiencies for representative exit velocities of the sweet and sour gases as calculated through eq 4. Calculated efficiencies were greatest for the sweet gas flare, with an exit velocity of 0.8 m/sec. Predicted combustion efficiencies for the sour gas flare were similar to those for the sweet gas flare, with an exit velocity of 3.1 m/sec. Figure 1 shows that combustion efficiency should be close to 100% at low wind speeds of ~1 m/sec and then decrease rapidly with increasing wind speed until at ~6 m/sec it begins to level off, to a value near 15%.

A comparison between predicted and observed combustion efficiencies as shown in Table 5 demonstrates generally good agreement. However, predicted values tended to be appreciably less than observed values at the relatively high wind speeds of 3.5 m/sec. There also seemed to be a tendency to overpredict efficiencies at low wind speeds.

#### CONCLUSIONS

The calculation results indicate that combustion efficiencies associated with flaring activity will be less for gases with high stoichiometric mixing ratios than for those with

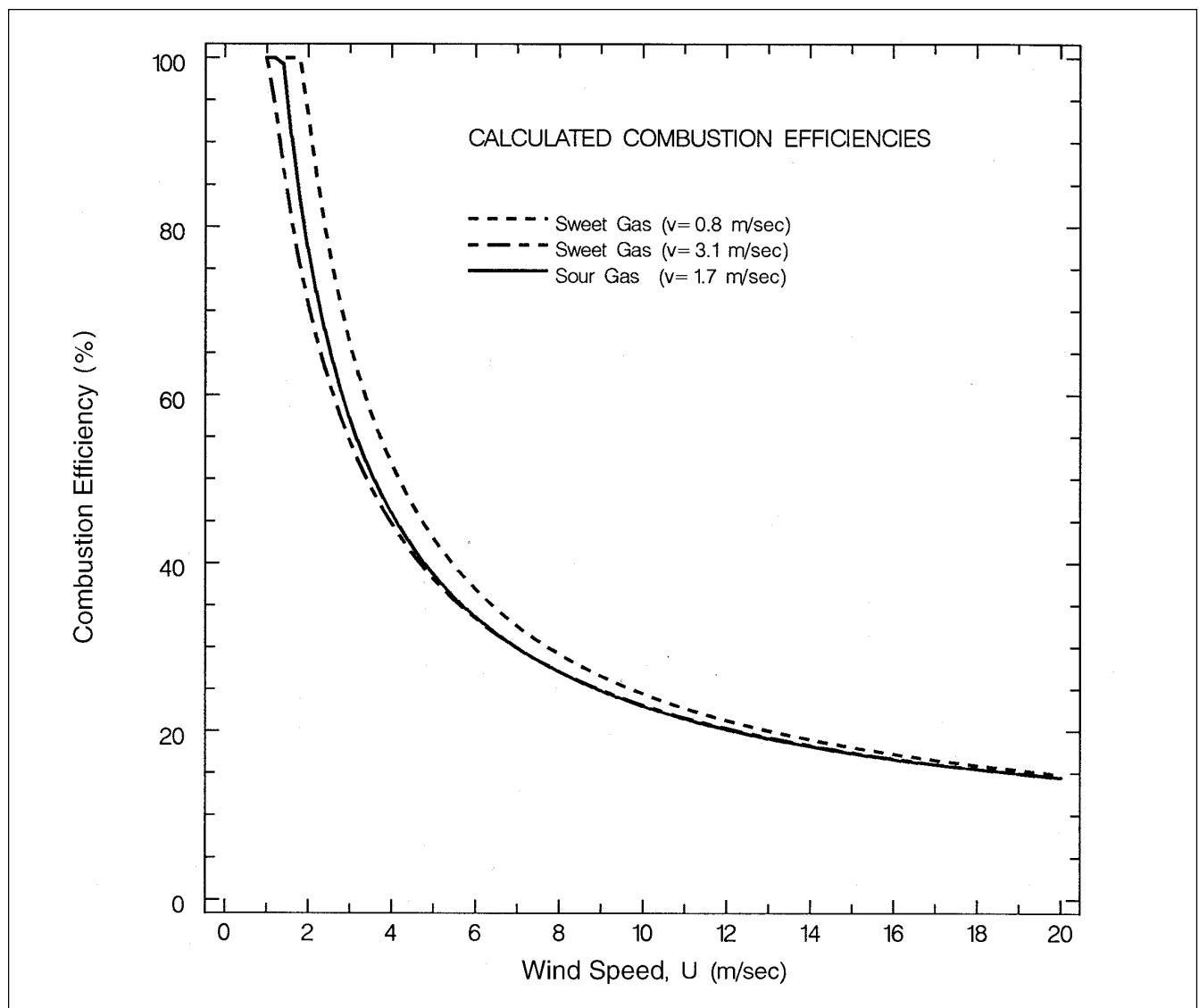
**Table 5.** Comparison between predicted and observed combustion efficiencies.

Observational Period	Wind Speed (m/sec)	Stack Exit Velocity (m/sec)	Combustion Efficiency (%)	
			Observed	Predicted
1	3.5	0.8	71	58
2	2.3	2.9	67	66
3	2.3	2.9	66	66
4	2.3	3.2	62	64
5	2.3	3.2	63	64
6	1.7	3.2	64	77
7	1.7	3.2	65	77
8	1.7	3.2	71	77
9	2.0	1.7	84	77
Average $\pm$ S.D. <sup>a</sup>	2.2 $\pm$ 0.6	2.7 $\pm$ 0.9	68 $\pm$ 7	69 $\pm$ 7

<sup>a</sup>S.D. = Standard deviation.

lower values. Combustion efficiencies will also tend to be sensitive to wind speeds and stack exit velocities. This is because a flame's area and volume are dependent on these variables, and it is the flame dimensions that must provide the means for dissipating the heat of combustion. A larger flame processes more fuel than does a smaller one.

Theoretical considerations and observational evidence suggest that flare combustion efficiencies typically may be ~70% at low wind speeds ( $U \leq 3.5$  m/sec). They should be even less at higher wind speeds. There were no observational data to assess the prediction of very low efficiencies of ~10% at high wind speeds. These predicted low efficiencies are indirectly verified, however, by the occurrence of flame blowout (i.e., zero combustion efficiency) during windy conditions.

**Figure 1.** Calculated combustion efficiency (%) as a function of wind speed for indicated stack exit velocities for sweet gas and sour gas.

Predictions for flare efficiencies as presented here are sensitive to the assumed flame temperature of 1200 K. For this reason, predicted efficiencies may depart appreciably from observed values. But limitations to the theoretical results imposed by this and other assumptions relating to plume dimensions should not be such as to obscure the main point of this paper: that the law of energy conservation appears to mandate that, all other things being equal, flame efficiencies must decrease as flame size decreases. Decreases in flame size occur in a significant manner with increasing stoichiometric mixing ratio, wind speeds, and stack exit velocities. All these parameters should therefore be considered in any assessment of a flare's ability to achieve high combustion efficiencies.

## REFERENCES

1. Boden, J.C.; Tjessem, K.; Wotton; A.G.; Moncrieff, J.T.M. *Petroleum Review* 1996, November, 524-528.
2. U.S. Environmental Protection Agency. *AP-42 Fifth Edition: Volume 1; Office of Air Quality Planning and Standards: Research Triangle Park, NC, 2000.*
3. Brzustowski, T.A. *22nd Canadian Chemical Engineering Conference*, Toronto, Ontario, Canada, September 17-22, 1972.
4. Brzustowski, T.A. *Prog. Energy Combust. Sci.* 1976, 2, 129-141.
5. Kent, G.P. *Hydrocarbon Process.* 1968, 47, 119-130.
6. Tan, S.H. *Hydrocarbon Process.* 1967, 46, 172-176.
7. Oenbring, P.R.; Sifferman, T.R. *Hydrocarbon Process.* 1980, 59, 124-129.
8. Leahey, D.M.; Paskall, H.G.; Schroeder, M.B.; Zelensky, M.J. *A Preliminary Study of the Chemical Composition and Combustion Efficiency of a Sour Gas Flare*; Alberta Environment, Research Management Division Report 85/30: Edmonton, Alberta, Canada, 1985.
9. Brzustowski, T.A. *Combust. Sci. Technol.* 1973, 6, 313-319.
10. Brzustowski, T.A. In *Proceedings of the Fifth Canadian Congress of Applied Mechanics*, Fredericton, Canada, May 26-30, 1975; pp 605-606.
11. Gollahalli, S.R. *Combust. Sci. Technol.* 1977, 15, 147-160.
12. Gollahalli, S.R.; Brzustowski, T.A.; Sullivan, H.F. *Trans. Canadian Soc. Mech. Eng.* 1975, 3, 205-214.
13. Becker, H.A.; Liang, D. *Combust. Flame* 1978, 32, 115-137.
14. Steward, F.R. *Combust. Sci. Technol.* 1970, 2, 203-212.
15. Beychok, M.R. *Fundamentals of Stack Gas Dispersion*; Milton R. Beychok, Irvine, CA, 1994.
16. Kalghatgi, G.T. *Combust. Flame* 1983, 52, 91-106.
17. Escudier, M.P. *Combust. Sci. Technol.* 1972, 4, 293-301.
18. Becker, H.A.; Liang, D.; Downey, C.I. In *Proceedings of the Eighteenth Symposium (International) on Combustion*; The Combustion Institute: Pittsburgh, PA, 1981; pp 1061-1071.
19. Leahey, D.M.; Schroeder, M.B. *Atmos. Environ.* 1987, 21, 777-784.
20. Leahey, D.M.; Schroeder, M.B. *Atmos. Environ.* 1990, 24A, 2527-2529.
21. Beychok, M.R. *Atmos. Environ.* 1987, 21, 1868.
22. Lewis, B.; Von Elbe, G. *Combustion Flames and Explosions of Gases*; Academic Press: New York, 1961; p 460.
23. Masliyeh, J.A.; Steward, F.R. *Combust. Flame* 1969, 13, 613-625.
24. Strosher, M. *Investigations of Flare Gas Emissions in Alberta*; Environmental Technologies, Alberta Research Council: Calgary, Alberta, Canada, 1996.
25. Strosher, M. *J. Air & Waste Manage. Assoc.* 2000, 50, 1723-1733.

## APPENDIX

Equations for flame dimensions (downwind extent, area, volume) as presented by Leahey et al.<sup>8</sup> and Leahey and Schroeder<sup>19,20</sup> are as follows:

$$x_f = 33 \frac{T R}{T_o C_s} h_f \quad (A1)$$

$$A_f = \frac{3927 D_o^2}{\beta_o C_s^2} \left[ \frac{T}{T_o} \right]^{\frac{3}{2}} \quad (A2)$$

$$V_f = \frac{7854 D_o^3}{\beta_o R^{\frac{1}{2}}} \left[ \frac{T}{T_o} \right]^{\frac{3}{2}} \left[ \frac{1}{C_s} \right]^{\frac{5}{2}} \quad (A3)$$

$$h_f = \frac{5 D_o}{0.4 + 1.2 R} \left[ \frac{T}{T_o C_s R} \right]^{\frac{1}{2}} \quad (A4)$$

$$\beta_o = 0.4 + 1.2 R \quad (A5)$$

$$R = \frac{U}{V} \quad (A6)$$

where  $A_f$  is the area of flame ( $m^2$ );  $D_o$  is the flare stack diameter (m);  $\beta_o$  is the entrainment parameter;  $C_s$  is the stoichiometric mixing ratio (%);  $T$  is the flame temperature (K);  $T_o$  is the ambient temperature (assumed to be 288 K);  $V_f$  is the volume of flame ( $m^3$ );  $R$  is the ratio of wind speed to stack exit velocity;  $x_f$  is the downwind extent of flame (m);  $h_f$  is the elevation of flame above the stack top (m);  $U$  is the wind speed (m/sec); and  $V$  is the stack exit velocity (m/sec).

### About the Authors

Douglas Leahey is principal scientist in the Air Quality Division at Jacques Whitford Environment Limited (JWEL), 703 - 6 Avenue S.W., Calgary, Alberta, Canada T2P 0T9. Katherine Preston is manager in the Air Quality Division at JWEL. Mel Strosher is a research officer with the Air Quality Assessment Group at the Alberta Research Council, 3608 - 33 Street N.W., Calgary, Alberta, Canada T2L 2A6.